



LUND UNIVERSITY
Faculty of Medicine

LUP

Lund University Publications

Institutional Repository of Lund University

This is an author produced version of a paper published in *Journal of Nuclear Cardiology* : official publication of the American Society of Nuclear Cardiology. This paper has been peer-reviewed but does not include the final publisher proof-corrections or journal pagination.

Citation for the published paper:
Helen Soneson, Henrik Engblom, Erik Hedström,
Frederic Bouvier, Peder Sörensson, John Pernow,
Håkan Arheden, Einar Heiberg

"An automatic method for quantification of myocardium at risk from myocardial perfusion SPECT in patients with acute coronary occlusion."

Journal of Nuclear Cardiology : official publication of the American Society of Nuclear Cardiology 2010 Jun
1

<http://dx.doi.org/10.1007/s12350-010-9237-z>

Access to the published version may require journal subscription.

Published with permission from: Elsevier

Title An Automatic Method for Quantification of Myocardium at Risk from Myocardial Perfusion SPECT in Patients with Acute Coronary Occlusion

Authors Helen Soneson MSc^{1,2}, Henrik Engblom MD PhD¹, Erik Hedström MD PhD¹, Frederic Bouvier MD PhD³, Peder Sörensson MD⁴, John Pernow MD PhD⁴, Håkan Arheden MD PhD¹, Einar Heiberg PhD¹

Author affiliation ¹Department of Clinical Physiology, Lund University, Skåne University Hospital, Lund, Sweden ²Numerical Analysis, Centre for Mathematical Sciences, Lund University, Lund, Sweden ³Department of Molecular Medicine and Surgery, Karolinska Institutet, Stockholm, Sweden ⁴Department of Medicine, Karolinska Institutet, Stockholm, Sweden

Corresponding Author Einar Heiberg, Department of Clinical Physiology, Lund University Hospital, SE-221 85 Lund, Sweden, Tel: +46-46-17 16 05
Fax: +46-46-15 17 69, einar.heiberg@med.lu.se

Financial support Swedish Heart Lung Foundation, Lund University Faculty of Medicine, the Swedish Research Council and the Region of Scania.

Abstract

Background: In order to determine myocardial salvage, accurate quantification of myocardium at risk (MaR) is necessary. We present a validated novel automatic segmentation algorithm for quantification of MaR by myocardial perfusion SPECT (MPS) in patients with acute coronary occlusion.

Methods and Results: Twenty-nine patients with coronary occlusion were injected with a perfusion tracer before reperfusion, and underwent rest MPS within 4 hours. The MaR was quantified using the proposed algorithm (Segment software), the software Quantitative Perfusion SPECT (QPS) and by manual segmentation. The Segment MaR algorithm used a threshold of 55% of maximal counts and an *a priori* model based on normal coronary artery perfusion territories. The MaR was 30 ± 10 % left ventricular mass (%LVM) by manual segmentation, 31 ± 12 %LVM by Segment and 36 ± 14 %LVM by QPS. There was a good agreement between automatic and manual segmentation for both of the algorithms with a lower bias for Segment (0.8 ± 4.0 %LVM) than for QPS (5.8 ± 5.8 %LVM) when compared to manual segmentation.

Conclusions: The Segment MaR algorithm can be used to correctly assess MaR from MPS images in patients with acute coronary occlusion without access to tracer-specific normal database. The MaR in relation to final infarct size enables determination of myocardial salvage.

Introduction

In patients with acute coronary occlusion, the myocardium supplied by the occluded artery will be subject to infarction if the blood flow is not restored. This region is referred to as the myocardium at risk (MaR) and can be quantified using myocardial perfusion SPECT (MPS)¹. Even though this patient population comprises a limited number of nuclear cardiology patients, MPS is considered the gold standard for quantification of MaR and has been used in both experimental² and human^{3, 4} studies by injecting the perfusion tracer during ongoing coronary occlusion. For fast and objective quantification of MaR, automatic computerized segmentation algorithms are needed. Quantification of MaR in relation to final infarct size enables determination of myocardial salvage accomplished by acute reperfusion therapy^{3, 5}.

The two most common ways for automatic quantification of perfusion defects by MPS are either using a normal template, based on counts of normal MPS examinations⁶⁻¹² or simple count thresholds¹³⁻¹⁵. The drawback with normal templates is the need for a normal database. This template can differ between systems due to the different camera settings and different tracers^{16, 17}. Another problem is the need of a co-registration between the template and the heart of each individual patient. When using simple threshold methods, myocardium with counts lower than a given threshold is defined as defects. Thus, by only using a threshold in the segmentation process, regions with low counts could potentially be incorrectly defined as defects, even though the low counts are caused by thinner myocardial wall, low spatial resolution or tissue attenuation.

The existing algorithms for segmentation of perfusion defects in MPS either require normal templates or the use of simple thresholds for the segmentation. Therefore, the aim of this study was to develop and validate a novel algorithm for quantification of MaR from MPS images that do not require a normal template and in addition to only using thresholds also

using a count normalization model and an *a priori* model based on the normal coronary artery perfusion territories.

Materials and Methods

Study population and design

All included patients and controls provided written informed consent to participate in the study and the study was approved by the regional ethics committee. The study consisted of two groups, 1) patients that underwent PCI due to coronary occlusion and 2) control subjects without cardiac disease.

Patients with coronary occlusion

Patient characteristics for the 29 included patients are shown in Table 1. Patients with chest pain, ST deviation on ECG suggesting acute myocardial ischemia, no history of prior infarction who underwent coronary artery angiography showing a single occlusion were included. Prior to opening of the occluded vessel the patients received a body weight-adjusted dose (350-700 MBq) of either ^{99m}Tc tetrofosmin (Myoview, Amersham Health, Buckinghamshire, UK) or sestamibi (MIBI, Cardiolite, Bristol Myers Squibb, USA). All patients underwent MPS within 3 and 4 hours, respectively. In the MPS images the MaR was quantified manually and by two automatic algorithms.

Control subjects

Ten control subjects (4 females and 6 males, 59 ± 6 years) with no history of or suspected cardiac disease were retrospectively included in the study. All control subjects were referred for MPS in the evaluation process for kidney donation. The control subjects received ^{99m}Tc tetrofosmin, with doses as described above, and underwent MPS within 3 hours.

Myocardial Perfusion SPECT acquisition and analysis

The MPS acquisition was performed at rest according to established clinical protocols using a dual head camera. The acquisition was performed at two different hospitals using three

different cameras; 11 patients were imaged with an ADAC Vertex (Milpitas, California, USA), 7 patients and the 10 control subjects with a GE Ventri (GE Healthcare, Buckinghamshire, UK) and 11 patients with a Sopha DST-XL (Sopha Medical Vision, Buc Cedex, France). The patients were placed in supine position and imaged in 32 or 64 projections over an 180° orbit using a 64x64 matrix. Total image acquisition time was approximately 15 minutes. The reconstructed voxel size was 3x3x3 mm (Sopha), 5x5x5 mm (ADAC) or 6.4x6.4x6.4 mm (GE). Iterative reconstruction was then performed on each camera as follows; The ADAC camera using maximum likelihood-expectation maximization (MLEM), with a Butterworth filter with a cutoff frequency set to 0.5 of Nyquist and order of 5.0. The GE camera using ordered subset expectation maximization (OSEM), with a Butterworth filter with a cutoff frequency set to 0.52 cycles/cm and order of 2.5. The Sopha camera using filtered back projection (FBP), with a Wiener filter with a power of 4.5. No attenuation or scatter correction was applied. Finally, short-axis images were reconstructed semi-automatically on the respective workstation for each camera.

The short-axis images of both the patients and the controls were loaded into the software Segment (v 1.8 R0923) ¹⁸. The left ventricle (LV) was automatically segmented according to the method described in ¹⁹. In short, the LV segmentation algorithm defines an optimal mid-mural centerline through the LV wall and on each side of this line the endocardium and epicardium are identified on the basis of an individually estimated wall thickness and counts thresholds. Two experienced observers, with 8 and 14 years of experience with MPS, respectively, manually improved the LV segmentation when necessary. For the patient population, the MaR was then manually segmented in consensus. The segmentation was performed in the original short-axis image and blinded to the results from the automatic MaR segmentations. For assessment of intraobserver variability of the manual segmentation of MaR, it was performed twice in 10 of the 29 patients, more than one month

after the consensus reading. An automated algorithm for segmentation of MaR was then applied as described in the next section.

Segmentation algorithm for myocardium at risk

The proposed algorithm for segmentation of MaR from short-axis MPS images, described in this study is implemented in the freely available software Segment (<http://segment.heiberg.se>)¹⁸. The algorithm is fully automatic and takes about 4 seconds to perform on an ordinary personal computer (3-GHz processor, 2 GB RAM). In summary, the algorithm starts by normalizing the counts in the myocardium in regions with underestimated counts. The algorithm then identifies all regions with counts below 55% of maximal counts in the myocardium. The next step in the algorithm is to apply an *a priori* model and finally refine the segmentation. The algorithm is described in detail in the following sections.

Counts normalization

The wall thickness of the basal and apical parts of the LV wall is normally thinner compared to the other parts of the LV wall. Thus, the perfusion in these regions may be underestimated due to low counts²⁰. To minimize incorrect segmentation of the MaR due to this underestimation, count normalization was performed in these short-axis slices. The counts in the basal slices were normalized so the highest values in the myocardium in each slice were equal to the highest value in the whole myocardium. The basal part was defined as the slices with outflow tract, according to the LV segmentation¹⁹. The most apical slice was normalized by the same value as the mean of the normalization values in the two most basal slices. The most apical parts cannot be used to set the normalization values since apical defects might result in complete absence of counts in the myocardium of the apical slices. The ability of the count normalization algorithm to compensate for normal count

variability in different parts of the myocardium was evaluated by comparing the count profile in the long axis direction before and after normalization in the control subjects.

Threshold segmentation

In the normalized image stack all pixels with counts below 55% of the maximal counts (mean of the three hottest pixels) in the LV were included in the threshold-based MaR segmentation. This threshold was derived from a recent ex-vivo experimental study²¹ where ex-vivo MPS images were fitted to ex-vivo MR images of pig hearts with coronary occlusion. The 55% threshold was identified as the mean percentage value of the maximal count at the MR image borders of the myocardium in the MPS image.

Applying the a priori model of the coronary distribution

To the threshold-based MaR segmentation an *a priori* model was then applied. The model was based on the distribution of single infarcts seen on biplane ventriculograms²² and divides the LV into 12 sections according to normal coronary artery territories. Figure 1a illustrates the model in a so called Mercator projection adapted and modified from a recently published study by Galeotti et al²³. From this Mercator projection a polar plot of the model was derived, as illustrated in Figure 1b. In the model, section 1 to 5 represent the region supplied by the left anterior descending coronary artery (LAD), section 6 to 9 by the left circumflex coronary artery (LCx) and section 8 to 12 by the right coronary artery (RCA). Sections 8 and 9 were included in both the LCx and the RCA regions due to variability in the normal coronary artery distribution between patients^{24, 25}. Threshold-based MaR segmentation that encompassed more than half of the volume in a section, or in the corresponding coronary region, was considered as MaR in the model-based segmentation. Segmentation that encompassed less than half of the volume in a section and in the corresponding region was excluded from the MaR segmentation. If the threshold-based segmentation extended outside the borders of an affected LV section into a neighboring

section, the volume close to the border was also included in the model-based segmentation to compensate for variability in coronary perfusion territories. For validation of the LV subdivision used in the *a priori* model, the MaR segmentation was also performed by using a standard 17-segment division of the LV²⁶.

Refinement of the segmentation

The model-based MaR segmentation was then refined considering anatomical and physiological assumptions of coronary artery supply of different parts of the myocardium. To avoid erroneous inclusion / exclusion of unphysiologically small islets within the MaR due to count irregularities the following four rules were defined prior to testing the segmentation algorithm: 1) In patients with coronary occlusion, the perfusion defect, and consequently the MaR, is assumed to only appear as transmural. This was performed by using the centerline method²⁷. The radial extent of the MaR segmentation was calculated along 100 chords, around the myocardium, perpendicular to the mid-mural centerline. In those directions where the MaR segmentation encompassed more than 60% of the wall thickness, all of the myocardium in that radial direction was included in the segmentation, which makes the MaR segmentation transmural in these directions. Consequently, in those directions where the MaR segmentation encompasses less than 60% of the wall thickness, the myocardium was not considered as MaR. 2) Small isolated islets (<100 mm²) with counts above the 55% threshold within the MaR segmentation in each short-axis slice were included in the segmentation. 3) Small regions of MaR segmentation, encompassing less than 10% of the myocardium in each short-axis slice, were excluded from the segmentation. 4) A region in a short-axis slice, excluded from the MaR segmentation, which had MaR segmentation in the corresponding region in the short-axis slice above and below were included in the segmentation.

The impact of the threshold for small isolated islets with count above the 55% threshold within the MaR and the impact of threshold for excluding small regions of MaR segmentation were tested by varying the thresholds as follows; By varying the area of small isolated islets from 0 mm² to 200 mm², a change in bias by 0.4 %LVM was found, and by varying the area of small regions from 5 % to 15 %, a change in bias by 1.5 %LVM was found. Thus, these thresholds were not critical to the bias and variability of the extent of MaR when comparing the automatic segmentation to manual segmentation. The impact from the four refinement steps on the final MaR was evaluated by performing the MaR segmentation without any of these steps and compared to manual segmentation.

Severity of the perfusion defect within the myocardium at risk

The final MaR segmentation was then applied to the original short-axis image stack from which severity of the perfusion defect within the MaR were calculated. Severity index was calculated as the severity of the MaR divided by the maximally possible severity²⁸ (Figure 2). The index was ranging from 0 (normal) to 100 (maximal severity). A total perfusion deficit (TPD) score, that takes both extent and severity for the MaR into account, was calculated as previously suggested by Slomka et. al.⁹. In short, TPD is calculated as;

$$TPD = 100 \times \frac{\sum_{i=0}^N score_i}{N}$$

where N was the total number of pixels within the myocardium in the short-axis image stack and $score$ was a continuous value assigned to each pixel. The $score$ was correlated to the severity and ranging from 0.5 (severity corresponding to the normal limit; 55% of maximal count in the LV) to 1 (severity corresponding to more than 70% below the normal limit) within the MaR and set to 0 in normal myocardium. This result in a TPD score ranging from 0 (normal) to 100 (maximal extent and severity). The TPD was calculated for both the entire LV as well as for each of the regions supplied by the three different coronary arteries as defined from the model in Figure 1. The TPD in section 8 and 9 in Figure 1,

which could belong to either the region supplied by LCx or by RCA, were associated to the region with the highest TPD.

Myocardium at risk by QPS

For comparison, the short-axis images were also loaded into the software Quantitative Perfusion SPECT (QPS 4.0; Cedars-Sinai Health System). The LV was automatically segmented by the program, with manual corrections of the approximate LV location in the image and the AV-plane position, when necessary. QPS then automatically defines MaR as regions in the LV with counts below a predefined standard deviation of a normal template of count values⁹. The normal template used in this study was the so called MibiMibi model in QPS, defined separately for females and males. Based on the segmentations, the QPS software quantified the extent of MaR as the percentage of abnormal myocardial pixels in the LV. The LV was divided into 17 segments by the QPS software, and in each of the segments the perfusion abnormality was graded on a 5-point scale, called the summed rest score (SRS). The SRS, ranging from 0 (normal) to 4 (maximum extent and severity), quantifies both extent and severity for the perfusion defect. The segments were automatically assigned to one of the three vascular territories; LAD, LCx or RCA, according to the 17-segment model, and the SRS were calculated for each of these regions. The SRS for each of the vascular territories was then used to validate the diagnostic accuracy by QPS for defining the occluded coronary artery compared to angiographic findings. The TPD by QPS was calculated according to the method by Slomka et al.⁹ as described above. The TPD by QPS was then compared to the TPD by Segment.

Statistical analysis

Values are presented as mean \pm SD. Pearson's linear regression analysis was performed to calculate the relationship between two variables. A P-value < 0.05 was considered statistically significant. The extent of MaR was expressed as percentage of total LV mass

(%LVM). The optimal cutoff point for the diagnostic accuracy for TPD by Segment and SRS by QPS for defining the occluded coronary artery compared to angiographic findings was obtained from analysis of receiver-operating characteristic (ROC) curve²⁹. A region that has higher or equal TPD and SRS than the cutoff point was considered as MaR, and a region with a score lower than the cutoff point was considered as normal.

Results

After automatic LV segmentation by Segment, the AV-plane position was manually corrected in 31% (9 out of 29) of the patients. For QPS, the approximate LV location in the image and the AV-plane position were manually corrected in 28% (8 out of 29) of the patients. Left ventricular mass by Segment was 139 ± 27 g (range 99-209 g) and by QPS 129 ± 30 g (range 88-192 g). All patients in the study had TIMI grade 0 flow seen on angiography.

Quantification of myocardium at risk

The result from the comparison of MaR between the two automatic segmentation algorithms and the manual segmentation is presented in Table 2 and Figure 3. The bias was lower for the Segment MaR algorithm than for QPS when compared to manual MaR segmentation ($p < 0.001$). The variability, however, did not differ statistically ($p = 0.055$). Figure 4 shows an example with automatic MaR segmentation by Segment and manual MaR segmentation in a patient with an LAD occlusion. In 28 % (8 out of 29) of the patients, QPS included small islets of myocardium with reduced counts in the MaR segmentation that was not included in the manual MaR segmentation. An example of this is shown in Figure 5. This was not seen in any of the patients for the MaR segmentation by Segment. For the manual segmentation of MaR the intraobserver variability was 0.4 ± 0.9 %LVM.

Total perfusion deficit by Segment and by QPS

The mean difference \pm SD between the Segment MaR algorithm and manual MaR segmentation for TPD was -0.6 ± 2.8 ($R^2 = 0.93$). The mean difference \pm SD between TPD by Segment and by QPS for the entire LV was -6.4 ± 5.7 ($R^2 = 0.86$, $p < 0.001$, Figure 6). Figure 7 shows the resulting ROC curve of diagnostic accuracy for TPD and SRS for

defining the occluded coronary artery by varying the cutoff point between 0 and 100. The area under the curve was 0.98 for the Segment MaR algorithm and 0.97 for QPS.

Validation of individual steps in the Segment MaR algorithm

The count normalization algorithm ability to compensate for normal count variability in different parts of the myocardium is illustrated for the control subjects in Figure 8, where the count profile in the long axis direction before and after normalization is shown. The SD for the counts in the myocardium was decreased, before compared to after the normalization algorithm was applied, from 15 % to 7.2 % in the male control subjects and from 16 % to 6.6 % in the female control subjects. By using a standard 17-segment model instead of the proposed division of the LV in the *a priori* model, the area under the curve in the ROC analysis was 0.97 when diagnostic accuracy for defining the occluded coronary artery was evaluated. By excluding the four refinement steps from the Segment MaR algorithm, the error between the automatic and manual MaR segmentation was 2.2 ± 4.1 %LVM, compared to 0.8 ± 4.0 when the refinement steps were included.

Discussion

This study shows good agreement for quantification and localization of MaR in MPS images in patients with coronary artery occlusion between fully automatic segmentation performed by the software Segment and manual segmentation.

Earlier algorithms using a threshold method for defining the perfusion defect of the LV using thresholds ranging from 45% to 60% of the maximum LV count^{13-15, 30}. All of these threshold values were derived from phantom studies. In this study the threshold value was taken from an animal study based on ex-vivo MR images and ex-vivo MPS images²¹.

Another improvement with the Segment MaR algorithm compared to earlier segmentation algorithms is the usage of a count normalization model and an *a priori* model based on normal coronary artery perfusion territories. This enables the algorithm to distinguish between physiologically plausible MaR from count loss due to i.e. a thinner myocardial wall in the basal and apical part of LV. Such a model has, to our knowledge, not been used before for this purpose. By using this model, the patients become their own controls and counts are not related to a normal material template that requires unique data bases for different tracers and protocols^{16, 17}. Furthermore, the Segment MaR algorithm performs the segmentation based on all counts in the myocardium which makes it less sensitive to noise and single hot pixels when compared to algorithms that only use the radial circumferential count maximum^{7, 10-13}.

There was a good agreement of MaR between the manual segmentation and both automatic algorithms. Compared to manual segmentation, however, the Segment MaR algorithm had lower bias than QPS. This could potentially be explained by QPS sometimes including small isolated regions as MaR. These regions were not included as MaR by manual segmentation or by the Segment MaR algorithm (Figure 5). Of notice, the Segment MaR

algorithm was specifically designed for segmentation of MaR in patients with occluded coronary arteries while QPS is designed for identification of varying degree of ischemia.

The Segment MaR algorithm has recently been used to reveal the time course of infarct evolution in relation to MaR in humans³, and has been shown to correlate with quantitative assessments of MaR using T2-weighted MR imaging⁴.

The TPD score by Segment provides information of both extent and severity of the MaR and show good correlation to the TPD score by QPS. Both TPD by Segment and SRS by QPS show high specificity and sensitivity in the diagnostic accuracy for defining the occluded coronary artery compared to angiographic findings.

Since both the LV segmentation and the following MaR segmentation in Segment is fully automatic, the reproducibility is high. Compared to manual segmentation, with both intra- and interobserver variability, the automatic algorithm produces the same result every time. Another advantage is that automatic segmentation is faster than manual segmentation. However, a manual interpretation is always required to distinguish between artefacts and MaR. Therefore, the automatic segmentation in Segment has been developed to easily allow for manual interactions when needed.

Study Limitations

No direct quantification of the “true” MaR was possible in this clinical study, in which manual segmentation by experienced observers was considered the gold standard. The limitation in the comparison between the two automatic segmentation softwares was that each of the software has their own LV segmentation. This can potentially lead to different conditions for the segmentation of MaR, especially in the basal region due to different definition of the most basal short-axis slice. However, this difference was minimized by

performing manual corrections of the LV segmentation in both softwares when necessary. The data was acquired by three different cameras and therefore have different voxel sizes, resulting in a heterogeneous dataset. On the other hand the Segment MaR algorithm performed equally well for all cameras which shows that the algorithm could potentially be used independent of vendor. The spatially uniform count compensation model was not designed to correct for tissue attenuation, but rather to compensate for the thin myocardium found in the most basal and apical parts of the left ventricle. The attenuation artifacts that results in localized areas with low counts are, however, accounted for by the subsequent refinement steps of the algorithm. In the present study, no patient was found where the Segment MaR algorithm failed due to attenuation artefacts. The refinement steps of the Segment MaR algorithm have a small impact on the quantitatively results of MaR. However, they are important for the visual impression of the segmentation. The *a priori* model of the coronary distribution in the algorithm was based on normal coronary artery perfusion territories in a right dominant model. The known variability regarding coronary supply of the inferolateral LV wall was however accounted for, which is not considered in the fixed standard 17-segment model. The proposed model of the LV division results in equally high diagnostic accuracy as the standard 17-segment model for defining the occluded coronary artery for the patients in this study, with a presumed variability of the coronary artery tree. Since the Segment MaR algorithm was developed for quantification of MaR, only patients with single occlusion and no patients with mild and stress-induced ischemia were included.

Conclusion

This study presents and validates a novel fully automatic segmentation algorithm for MaR from MPS images in patients with acute coronary occlusion. Although no automatic method should be used without manual inspection, we believe that this segmentation algorithm could be a useful tool for faster, more reproducible and observer independent

assessment of MaR in MPS images, which enables assessment of myocardial salvage when compared to final infarct size.

Acknowledgements

The authors would like to thank technicians Ann-Helen Arvidsson and Christel Carlander for invaluable help with data acquisition. Funding for this project come in part from the Swedish Heart Lung Foundation, Sweden, Lund University Faculty of Medicine, Lund Sweden, the Swedish Research Council, Sweden and the Region of Scania, Sweden.

Table 1. Patient characteristics

Characteristic	Number	%
Male gender	23	79
Female gender	6	21
Age (y)	65±10 (36-83)	
LAD occlusion	9	31
LCx occlusion	1	3
RCA occlusion	19	66

LAD = left anterior descending coronary artery, LCx = left circumflex coronary artery,

RCA = right coronary artery.

Table 2. Result from the comparison between the two automatic MaR segmentation algorithms and manual MaR segmentation.

	Patient group (number of patients)	Manual MaR segmentation	MaR segmentation by Segment	MaR segmentation by QPS
MaR (%LVM)	All (29)	30 ± 10 (range 13 – 52)	31 ± 12 (range 5.3 – 55)	36 ± 14 (range 10 – 65)
	LAD (9)	41 ± 7.3 (range 33 – 52)	42 ± 7.4 (range 33 – 55)	50 ± 8.8 (range 37 – 65)
	LCx (1)	27	42	36
	RCA (19)	25 ± 7.5 (range 13 – 40)	25 ± 9.3 (range 5.3 – 41)	29 ± 12 (range 10 – 58)
Error MaR (%LVM)	All (29)	-	0.8 ± 4.0	5.8 ± 5.8
	LAD (9)	-	0.9 ± 2.8	9.4 ± 5.1
	LCx (1)	-	15	9
	RCA (19)	-	0.0 ± 3.0	4.0 ± 5.5

The error MaR is the difference between the automatic MaR segmentation algorithm and the manual MaR segmentation. LAD = left anterior descending coronary artery, LCx = left circumflex coronary artery, RCA = right coronary artery.

Figure 1. Illustration of the *a priori* model of the LV shown in Mercator projection (a) and as a polar plot (b). The model was adapted and modified from Galeotti et al.²³ with permission. The LV was divided into 12 sections based on normal coronary artery perfusion territories. Section 1-5 is supplied by the left anterior descending coronary artery (LAD), section 6-9 by the left circumflex coronary artery (LCx) and section 8-12 by the right coronary artery (RCA). Section 8 and 9 were included in both the LCx and the RCA region.

Figure 2. Count profile for one short-axis slice with MaR in the lateral/inferior wall. The light shaded region (A) is the severity of the defect in this slice. The light shaded (A) + the dark shaded (B) region is the maximally possible severity. Severity index was calculated as $A/(A+B)$.

Figure 3. The relationship between MaR assessed automatically and by manual segmentation. a) Relationship between MaR by Segment and by manual segmentation. The dashed line is the line of identity. b) Relationship between MaR by QPS and by manual segmentation. The dashed line is the line of identity. c) Relationship between error in MaR, for Segment, and manual segmentation. d) Relationship between error in MaR, for QPS, and manual segmentation. There was a good agreement between automatic and manual segmentation for both of the algorithms with a lower bias for Segment than for QPS when compared to manual segmentation.

Figure 4. Short-axis images with segmentation of MaR by Segment (a) and by manual segmentation (b) in one patient with an LAD occlusion. Myocardium at risk was 39 %LVM by the Segment MaR algorithm and 37 %LVM by manual segmentation. The white lines represent the myocardial borders and the dashed regions the MaR. There was a good agreement between segmentation performed by the Segment MaR algorithm and manual

segmentation for both extent and location of the MaR. Note the attenuation artifact in the basal part of the inferior LV wall (arrows) that neither the Segment MaR algorithm nor the experienced observers included in the MaR segmentation.

Figure 5. Illustration of the LV and MaR segmentations in one patient with an RCA occlusion. In the upper panel the long-axis images in both the horizontal and vertical direction with LV segmentation from each software is presented. The middle and lower panel illustrates polar plots with the counts in the myocardium and the MaR segmentation, respectively. In the lower panel the black region represents the MaR. The extent of MaR was quantified as 28 %LVM by manual segmentation, 30 %LVM by Segment and 36 %LVM by QPS. The overestimation of MaR by QPS in this case, can partially be explained by the small isolated regions of MaR segmentation in the anterolateral part of the LV. This region was not included by the Segment MaR algorithm or for the manual MaR segmentation.

Figure 6. Relationship between TPD, which includes both extent and severity of the MaR, by Segment and by QPS. There was a good correlation between the scores from the two algorithms.

Figure 7. Receiver-operating characteristic curve of diagnostic accuracy for TPD by Segments and SRS by QPS for defining the occluded coronary artery compared to angiographic findings. Area under the curve was 0.98 and 0.97 for Segment and QPS, respectively. The point on the ROC curve closest to the upper left corner was for Segment corresponding to a sensitivity of 0.93 and a specificity of 0.98 (red circle, cutoff point = 19) and for QPS a sensitivity of 0.90 and a specificity of 0.95 (green circle, cutoff point = 11).

Figure 8. Mean myocardial counts in each short-axis slice for the control subjects before and after the count normalization model was applied. The model was compensating for the count loss in the basal and apical part of the LV due to thinner myocardial wall in these regions.

References

1. Gibbons RJ, Miller TD, Christian TF. Infarct size measured by single photon emission computed tomographic imaging with (99m)Tc-sestamibi: A measure of the efficacy of therapy in acute myocardial infarction. *Circulation*. 2000;101:101-8.
2. Gotberg M, Olivecrona GK, Engblom H, Ugander M, van der Pals J, Heiberg E, et al. Rapid short-duration hypothermia with cold saline and endovascular cooling before reperfusion reduces microvascular obstruction and myocardial infarct size. *BMC Cardiovasc Disord*. 2008;8:7.
3. Hedström E, Engblom H, Frogner F, Åström-Olsson K, Öhlin H, Jovinge S, et al. Infarct evolution in man studied in patients with first-time coronary occlusion in comparison to different species - implications for assessment of myocardial salvage. *J Cardiovasc Magn Reson*. 2009;11:38.
4. Carlsson M, Ubachs JF, Hedstrom E, Heiberg E, Jovinge S, Arheden H. Myocardium at risk after acute infarction in humans on cardiac magnetic resonance: quantitative assessment during follow-up and validation with single-photon emission computed tomography. *JACC Cardiovasc Imaging*. 2009;2:569-76.
5. Ortiz-Perez JT, Meyers SN, Lee DC, Kansal P, Klocke FJ, Holly TA, et al. Angiographic estimates of myocardium at risk during acute myocardial infarction: validation study using cardiac magnetic resonance imaging. *Eur Heart J*. 2007;28:1750-8.
6. Benoit T, Vivegnis D, Foulon J, Rigo P. Quantitative evaluation of myocardial single-photon emission tomographic imaging: application to the measurement of perfusion defect size and severity. *Eur J Nucl Med*. 1996;23:1603-12.
7. Garcia EV, Van Train K, Maddahi J, Prigent F, Friedman J, Areeda J, et al. Quantification of rotational thallium-201 myocardial tomography. *J Nucl Med*. 1985;26:17-26.
8. Kang X, Berman DS, Van Train KF, Amanullah AM, Areeda J, Friedman JD, et al. Clinical validation of automatic quantitative defect size in rest technetium-99m-sestamibi myocardial perfusion SPECT. *J Nucl Med*. 1997;38:1441-6.
9. Slomka PJ, Nishina H, Berman DS, Akincioglu C, Abidov A, Friedman JD, et al. Automated quantification of myocardial perfusion SPECT using simplified normal limits. *J Nucl Cardiol*. 2005;12:66-77.
10. Nuyts J, Mortelmans L, Suetens P, Oosterlinck A, de Rou M. Model-based quantification of myocardial perfusion images from SPECT. *J Nucl Med*. 1989;30:1992-2001.
11. DePasquale EE, Nody AC, DePuey EG, Garcia EV, Pilcher G, Bredlau C, et al. Quantitative rotational thallium-201 tomography for identifying and localizing coronary artery disease. *Circulation*. 1988;77:316-27.
12. Van Train KF, Areeda J, Garcia EV, Cooke CD, Maddahi J, Kiat H, et al. Quantitative same-day rest-stress technetium-99m-sestamibi SPECT: definition and

validation of stress normal limits and criteria for abnormality. *J Nucl Med.* 1993;34:1494-502.

13. Gibbons RJ, Verani MS, Behrenbeck T, Pellikka PA, O'Connor MK, Mahmorian JJ, et al. Feasibility of tomographic ^{99m}Tc-hexakis-2-methoxy-2-methylpropyl-isonitrile imaging for the assessment of myocardial area at risk and the effect of treatment in acute myocardial infarction. *Circulation.* 1989;80:1277-86.

14. Ibrahim T, Nekolla SG, Hornke M, Bulow HP, Dirschinger J, Schomig A, et al. Quantitative measurement of infarct size by contrast-enhanced magnetic resonance imaging early after acute myocardial infarction: comparison with single-photon emission tomography using Tc^{99m}-sestamibi. *J Am Coll Cardiol.* 2005;45:544-52.

15. Tamaki S, Nakajima H, Murakami T, Yui Y, Kambara H, Kadota K, et al. Estimation of infarct size by myocardial emission computed tomography with thallium-201 and its relation to creatine kinase-MB release after myocardial infarction in man. *Circulation.* 1982;66:994-1001.

16. Germano G, Kavanagh PB, Waechter P, Areeda J, Van Kriekinge S, Sharir T, et al. A new algorithm for the quantitation of myocardial perfusion SPECT. I: technical principles and reproducibility. *J Nucl Med.* 2000;41:712-9.

17. Van Train KF, Maddahi J, Berman DS, Kiat H, Areeda J, Prigent F, et al. Quantitative analysis of tomographic stress thallium-201 myocardial scintigrams: a multicenter trial. *J Nucl Med.* 1990;31:1168-79.

18. Heiberg E, Sjogren J, Ugander M, Carlsson M, Engblom H, Arheden H. Design and validation of Segment - freely available software for cardiovascular image analysis. *BMC Med Imaging.* 2010;10:1.

19. Sonesson H, Ubachs JF, Ugander M, Arheden H, Heiberg E. An Improved Method for Automatic Segmentation of the Left Ventricle in Myocardial Perfusion SPECT. *J Nucl Med.* 2009;50:205-13.

20. Mahrholdt H, Zhydkov A, Hager S, Meinhardt G, Vogelsberg H, Wagner A, et al. Left ventricular wall motion abnormalities as well as reduced wall thickness can cause false positive results of routine SPECT perfusion imaging for detection of myocardial infarction. *Eur Heart J.* 2005;26:2127-35.

21. Ugander M, Sonesson H, Heiberg E, Engblom H, Pals Jvd, Erlinge D, et al. A novel method for quantifying myocardial perfusion SPECT defect size by co-registration and fusion with MRI - an experimental ex vivo imaging pig heart study. Paper presented at: X Cardiovascular Spring Meeting, 2008; Malmö.

22. RH Selvester, GS Wagner, RE Ideker. *Myocardial infarction.* Vol 1. New York: Pergamon Press; 1989.

23. Galeotti L, Strauss DG, Ubachs JF, Pahlm O, Heiberg E. Development of an automated method for display of ischemic myocardium from simulated electrocardiograms. *J Electrocardiol.* 2009;42:204-12.

24. Persson E, Palmer J, Pettersson J, Warren SG, Borges-Neto S, Wagner GS, et al. Quantification of myocardial hypoperfusion with ^{99m}Tc-sestamibi in patients

undergoing prolonged coronary artery balloon occlusion. *Nucl Med Commun.* 2002;23:219-28.

25. Pereztol-Valdes O, Candell-Riera J, Oller-Martinez G, Aguade-Bruix S, Castell-Conesa J, Angel J, et al. [Localization and quantification of myocardium at risk by myocardial perfusion SPECT during coronary artery occlusion]. *Rev Esp Cardiol.* 2004;57:635-43.

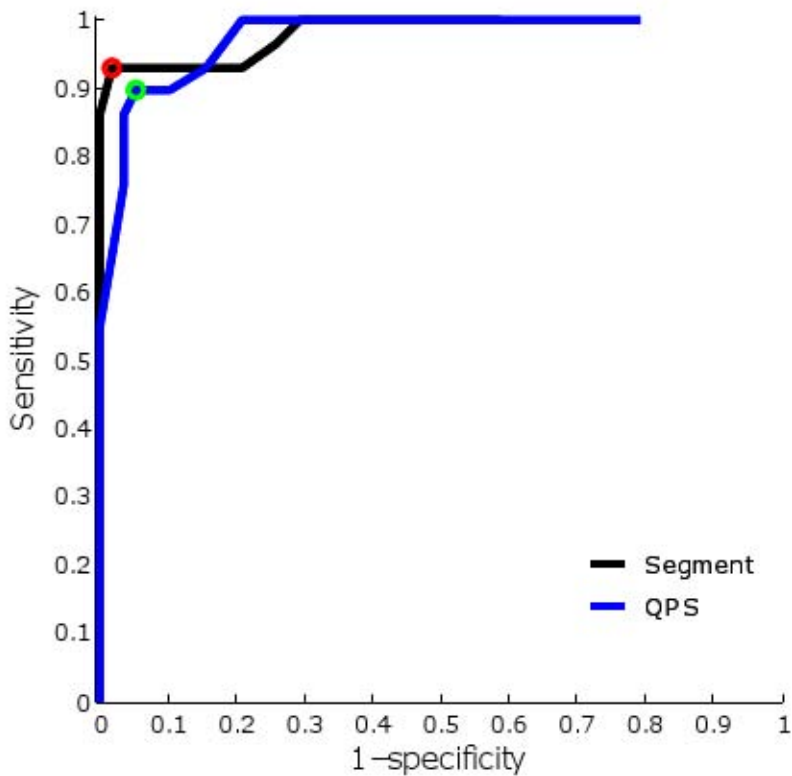
26. Cerqueira MD, Weissman NJ, Dilsizian V, Jacobs AK, Kaul S, Laskey WK, et al. Standardized myocardial segmentation and nomenclature for tomographic imaging of the heart: a statement for healthcare professionals from the Cardiac Imaging Committee of the Council on Clinical Cardiology of the American Heart Association. *Circulation.* 2002;105:539-42.

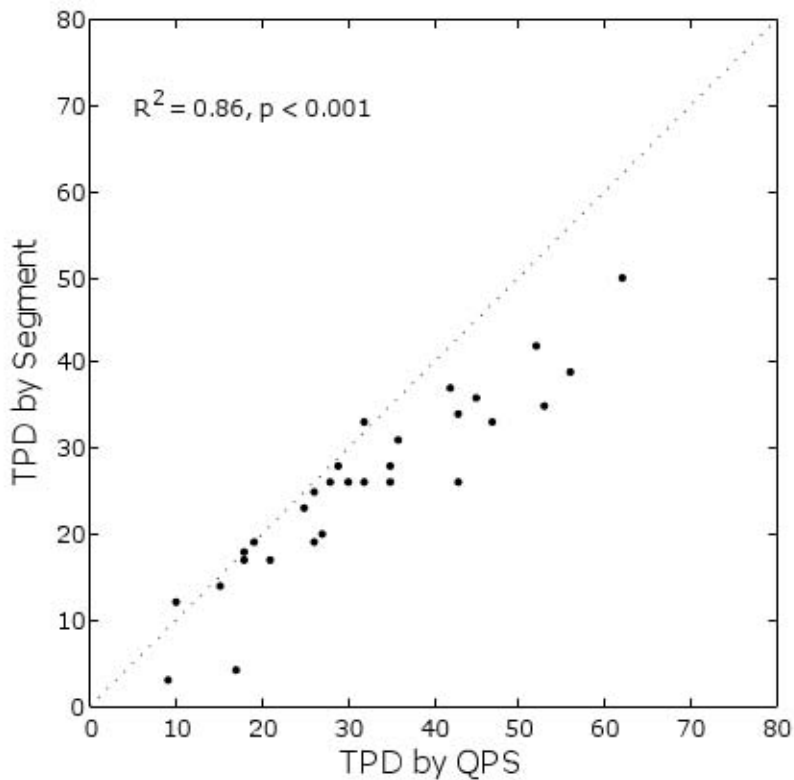
27. Sheehan FH, Bolson EL, Dodge HT, Mathey DG, Schofer J, Woo HW. Advantages and applications of the centerline method for characterizing regional ventricular function. *Circulation.* 1986;74:293-305.

28. Christian TF, Schwartz RS, Gibbons RJ. Determinants of infarct size in reperfusion therapy for acute myocardial infarction. *Circulation.* 1992;86:81-90.

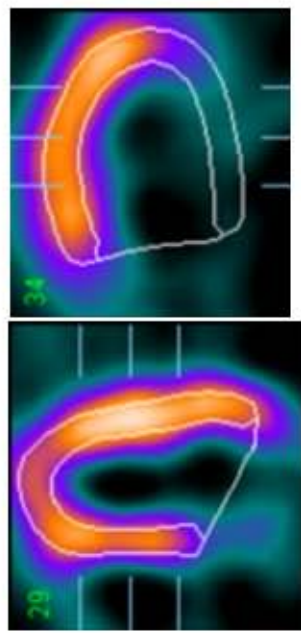
29. Altman DG, Bland JM. Diagnostic tests 3: receiver operating characteristic plots. *Bmj.* 1994;309:188.

30. Mortelmans L, Nuyts J, Vanhaecke J, Verbruggen A, De Roo M, De Geest H, et al. Experimental validation of a new quantitative method for the analysis of infarct size by cardiac perfusion tomography (SPECT). *Int J Card Imaging.* 1993;9:201-12.

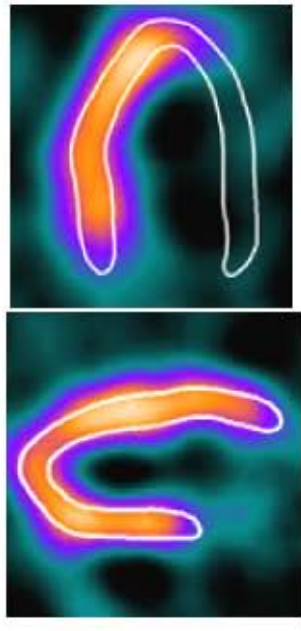




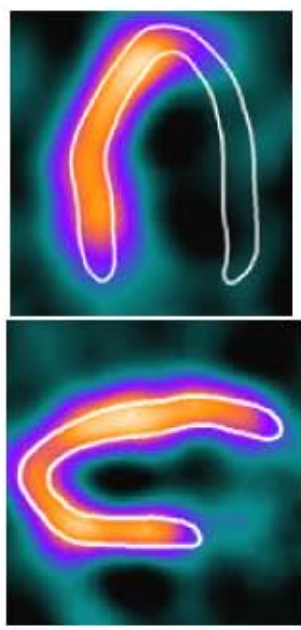
QPS



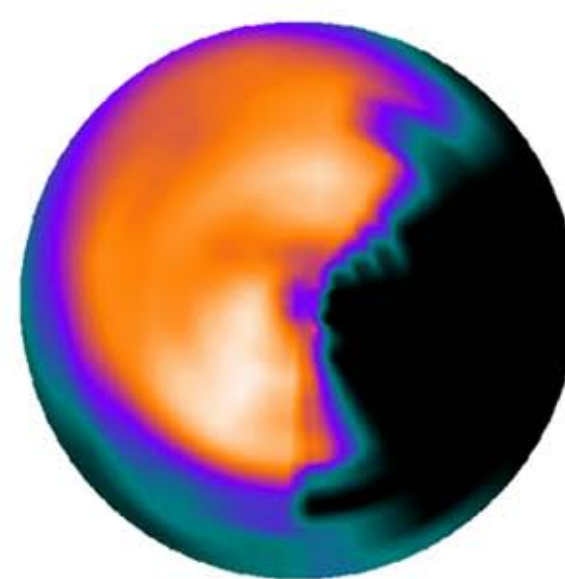
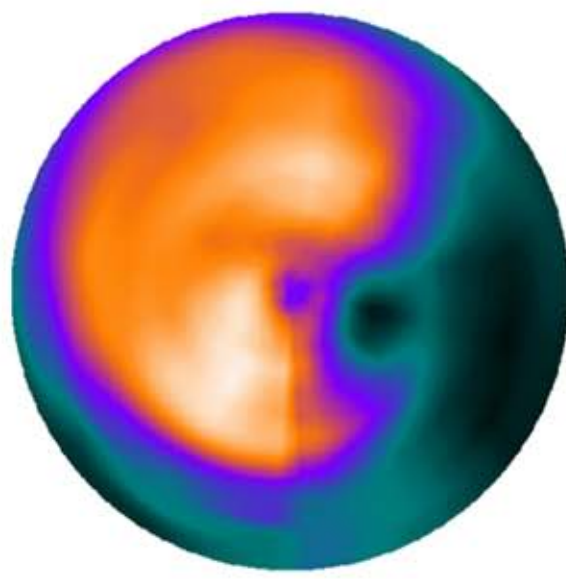
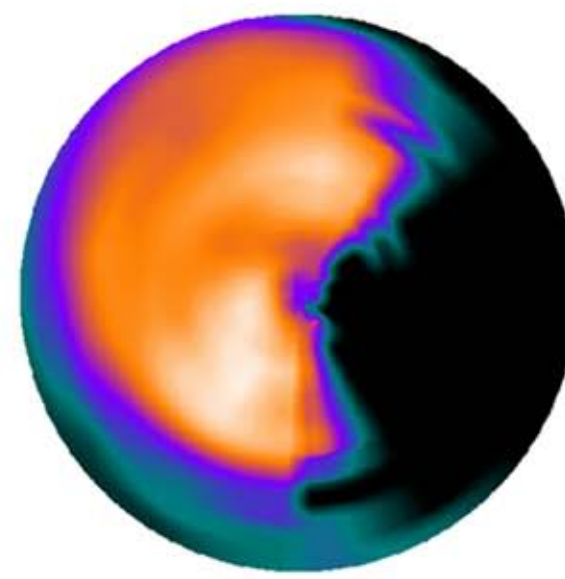
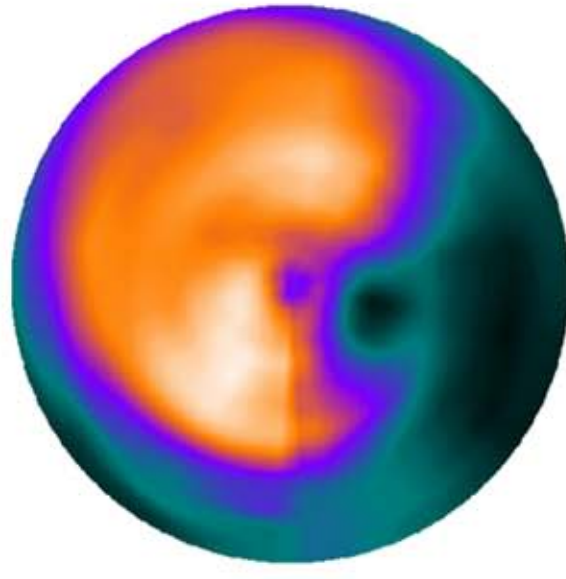
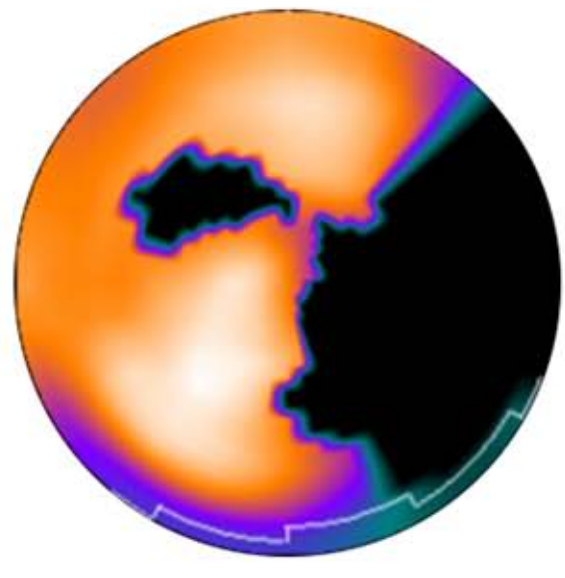
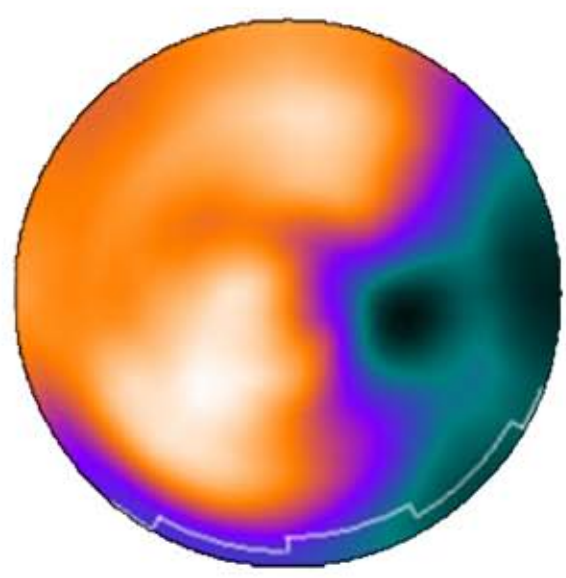
Segment



Manual segmentation



LV segmentation



Counts

MaR

a**b**

